REPORT DOCUMENTATION PAGE

Form Approved OMB NO. 0704-0188

1. REPORT DATE (DD-MM-YYYY)	2. REPORT TYPE	3. DATES COVERED (From - To)
19-12-2011	Final Report	15-Jul-2010 - 14-Jul-2011

4. TITLE AND SUBTITLE

Metatronics for Ultra-High-Speed Low-Power Nano-Circuits

5a. CONTRACT NUMBER

W911NF-10-1-0310

5b. GRANT NUMBER

5c. PROGRAM ELEMENT NUMBER

0D10BG

6. AUTHORS

Edo Waks, Sangbok Lee, Nader Engheta, Benjamin Shapiro

5d. PROJECT NUMBER

5e. TASK NUMBER

5f. WORK UNIT NUMBER

7. PERFORMING ORGANIZATION NAMES AND ADDRESSES

University of Maryland - College Park
Research Admin. & Advancement
University of Maryland
College Park, MD 20742 -5141

8. PERFORMING ORGANIZATION REPORT NUMBER

9. SPONSORING/MONITORING AGENCY NAME(S) AND ADDRESS(ES)

U.S. Army Research Office
P.O. Box 12211
Research Triangle Park, NC 27709-2211

10. SPONSOR/MONITOR'S ACRONYM(S)

ARO

11. SPONSOR/MONITOR'S REPORT NUMBER(S)

58315-MS-DRP.2

12. DISTRIBUTION AVAILIBILITY STATEMENT

Approved for Public Release; Distribution Unlimited

13. SUPPLEMENTARY NOTES

The views, opinions and/or findings contained in this report are those of the author(s) and should not contrued as an official Department of the Army position, policy or decision, unless so designated by other documentation.

14. ABSTRACT

The PIs have investigated methods to integrate plasmonic and dielectric nanoparticles with flow control to develop complex nanosystems for devlopment of ultra-fast electronic circuits.

15. SUBJECT TERMS

Nanophotonics, plasmonics, nanoelectronics, quantum optics

16. SECURITY CLASSIFICATION OF:			17. LIMITATION OF ABSTRACT	15. NUMBER OF PAGES	19a. NAME OF RESPONSIBLE PERSON
a. REPORT	b. ABSTRACT	c. THIS PAGE			Edo Waks
UU	UU	UU	UU		19b. TELEPHONE NUMBER: 301-405-5022

Report Title

Metatronics for Ultra-High-Speed Low-Power Nano-Circuits

ABSTRACT

The PIs have investigated methods to integrate plasmonic and dielectric nanoparticles with flow control to develop complex nanosystems for devlopment of ultra-fast electronic circuits.

Enter List of papers submitted or published that acknowledge ARO support from the start of the project to the date of this printing. List the papers, including journal references, in the following categories:

(a) Papers published in peer-reviewed journals (N/A for none)

Received Paper

TOTAL:

Number of Papers published in peer-reviewed journals:

(b) Papers published in non-peer-reviewed journals (N/A for none)

Received Paper

TOTAL:

Number of Papers published in non peer-reviewed journals:

(c) Presentations

Number of Presentations: 3.00

Non Peer-Reviewed Conference Proceeding publications (other than abstracts):

Received Paper

TOTAL:

Number of Non Peer-Reviewed Conference Proceeding publications (other than abstracts):

Peer-Reviewed Conference Proceeding publications (other than abstracts):

Received Paper

TOTAL:

Number of Peer-Reviewed Conference Proceeding publications (other than abstracts):

(d) Manuscripts

Received Paper

TOTAL:

Number of Manuscripts:

Books

Received Paper

TOTAL:

Patents Submitted

Patents Awarded

Awards

Graduate Students

NAME	PERCENT_SUPPORTED	Discipline
Chad Ropp	0.25	
FTE Equivalent:	**0.25**	
Total Number:	**1**	

Names of Post Doctorates

NAME	PERCENT_SUPPORTED
FTE Equivalent:	
Total Number:	

Names of Faculty Supported

NAME	PERCENT_SUPPORTED
FTE Equivalent:	
Total Number:	

Names of Under Graduate students supported

NAME	PERCENT_SUPPORTED
FTE Equivalent:	
Total Number:	

Student Metrics

This section only applies to graduating undergraduates supported by this agreement in this reporting period

The number of undergraduates funded by this agreement who graduated during this period:	1.00
The number of undergraduates funded by this agreement who graduated during this period with a degree in science, mathematics, engineering, or technology fields:.....	1.00
The number of undergraduates funded by your agreement who graduated during this period and will continue to pursue a graduate or Ph.D. degree in science, mathematics, engineering, or technology fields:.....	1.00
Number of graduating undergraduates who achieved a 3.5 GPA to 4.0 (4.0 max scale):	0.00
Number of graduating undergraduates funded by a DoD funded Center of Excellence grant for Education, Research and Engineering:	0.00
The number of undergraduates funded by your agreement who graduated during this period and intend to work for the Department of Defense	0.00
The number of undergraduates funded by your agreement who graduated during this period and will receive scholarships or fellowships for further studies in science, mathematics, engineering or technology fields:	0.00

Names of Personnel receiving masters degrees

NAME

Total Number:

Names of personnel receiving PHDs

NAME

Total Number:

Names of other research staff

NAME PERCENT_SUPPORTED

FTE Equivalent:

Total Number:

Sub Contractors (DD882)

Inventions (DD882)

Scientific Progress

Technology Transfer

Integration of QDs with plasmonic nanoparticles

We have developped a unique capability to integrate plasmonic nanoparticles with single QDs as a method to assemble nanoelectronic circuits. An optical image of the microfluidic device used to position QDs is shown in Fig. 1a. Four tapered microfluidic channels intersect at the control region where QD manipulation occurs (the dashed circle). AgNWs with an average diameter of 100 nm and an average length of 4 μm (SEM image in Fig. 1c inset) are deposited on the polydimethylsiloxane (PDMS) surface of the control region. The channels are filled with fluid containing QDs that become confined to a thin sheath along the surface due to the fluid chemistry. Within this sheath, QDs are manipulated to nanometric precision using electroosmosis with feedback control. The AgNW acts as an obstacle for the QDs, indicating that they are constrained to lie within 100 nm of the surface (the height of the AgNW). The device is mounted on an inverted microscope and QDs are imaged using a CCD camera. Their positions are tracked with sub-wavelength precision by fitting the diffraction spot to a Gaussian point spread function. The vision accuracy of the QD tracking algorithm was determined to be 9 nm by tracking an immobilized QD on a glass surface

Fig. 1b. illustrates how imaging of an AgNW is performed. Within the control region, a single QD is selected and driven along a trajectory that samples the local field of the wire at a desired set of locations. The accuracy within which QDs can be positioned is measured to be 41 nm, ensuring that we can deterministically probe the wire mode at a desired location on-demand. The QD trajectory is selected to maximize data sampling near the wire surface. Figs. 1c-e are a series of images of a single QD being moved progressively closer to an AgNW. When the QD is in close proximity to the wire, light scatter is observed from the wire ends (Fig. 1e). A collection of such images can be used to map the SPP mode of the AgNW by monitoring the scattered intensity at the ends of the nanowire as a function of the QD position.

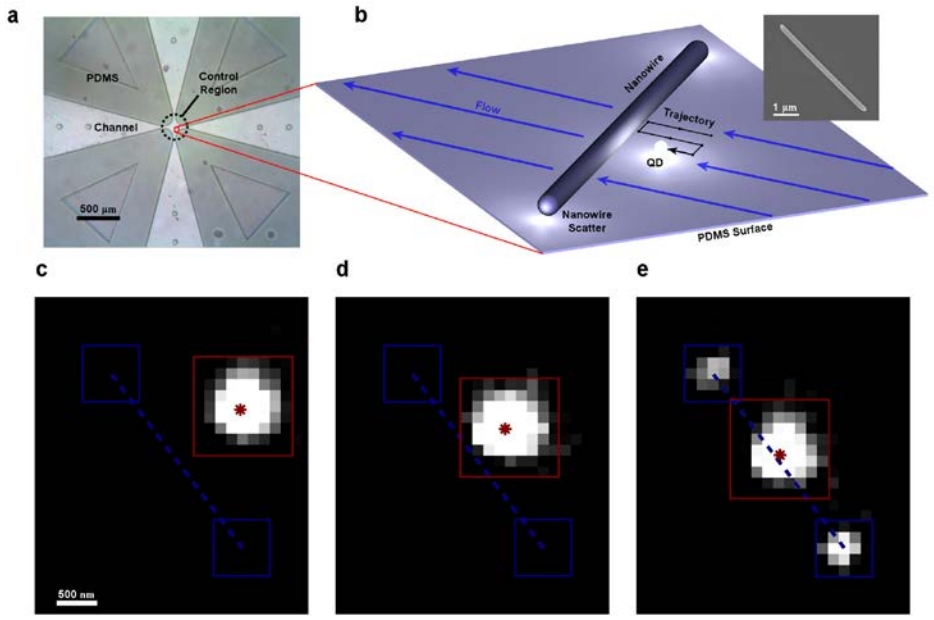

Figure 1 | QD near-field probing. **a.** Optical image of the microfluidic crossed-channel device. **b.** Illustration of positioning and imaging technique. **c-e**. A series of emission images showing coupling of the QD to the AgNW as the QD is moved closer to the wire.

Fig. 2a shows a scan of our probing technique used to measure the mode of a silver nanowire. The shaded region represents the wire location as estimated from light scattered from the wire ends and an assumed AgNW radius of 50 nm. The color of each data point corresponds to the intensity at that location, which is observed to increase as the QD approaches the AgNW. Fig. 2b plots the imaging intensity as a function of radial distance from the wire axis. The solid blue line in Fig. 2b is the Bessel-function fit and the red dashed line corresponds to the AgNW evanescent field as calculated using finite-difference time-domain (FDTD) simulation (see Methods).

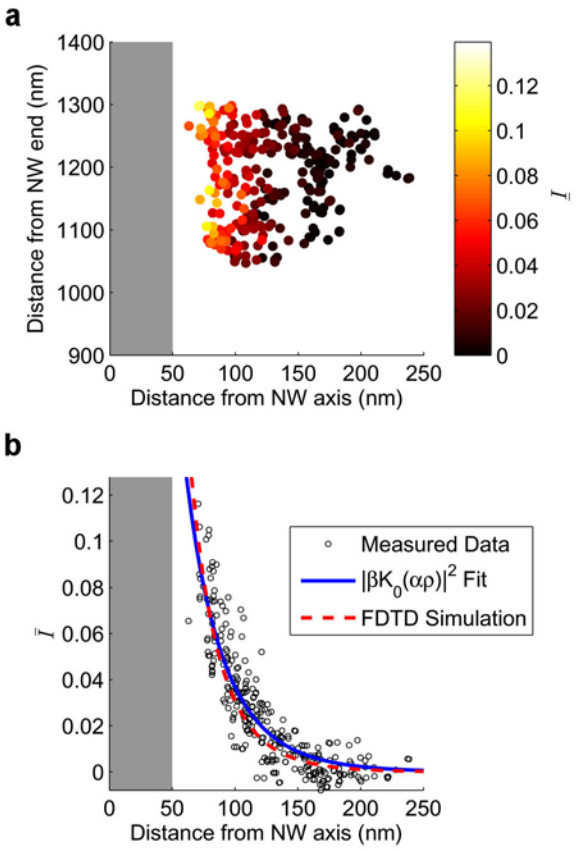

Figure 2 | Probing the evanescent field of an AgNW. a. $\bar{I}$ as a function of position near the middle of the wire. The shaded area indicates the physical extent of the AgNW. **b.** $\bar{I}$ as a function of distance from wire axis using data from panel a. The blue line indicates the best fit to a modified Bessel function. The red line is an FDTD simulation of the AgNW evanescent field. The simulation result was fit to the data using an overall scaling factor.

The demonstrated probing technique shows that we can couple single nanoparticles to nanowires for integration. This method provides a promising approach towards development of metactronic circuits that could enable Terahertz computation. We have also incorporated methods for immobilizing the QDs on the wires for development of nano-devices.

Nonlinear generation of light in plasmonics

One issue in the development of metactronic devices is coupling light from the far field into the devices. For instance, for devices based on metal nanowires, coupling light in from the far field is challenging because momentum matching conditions must be met from the far field into the surface plasmon polariton (SPP) mode, which is best accomplished when the light propagates along the nanowire. However, in this case the polarization is not appropriate for coupling. To address this issue, we developed a method of preparing tapered metal nanowires. The process involves electrochemical synthesis of long silver nanowires in an alumina template, with one end of each nanowire adiabatically tapered to a diameter of tens of nanometers. Measurements show that far-field photons can couple into the tapered end, and conversely that SPPs couple efficiently from the tapered end into the far field.

We further demonstrated that when the end of a metal nanowire is irradiated in the far field with ultrafast pulses of near-infrared radiation, broadband visible luminescence is generated. Because the luminescence is generated within the nanowire, the excited region acts as a near-field source that can couple the broadband radiation efficiently into the SPP mode of the nanowire. This phenomenon, which we call guided multiphoton-absorption-induced luminescence (GMAIL), allows us to use nanowires as the basis for broadband optical devices. Furthermore, because the SPP mode becomes leaky at the junction of a nanowire and another nanostructure (such as a quantum dot), we can perform photochemistry selectively at such a junction. By combining this phenomenon with electroosmotic flow control, we have demonstrated the precision, on-demand assembly of quantum dots to silver nanowires.

We have also prepared silver nanowires with ~25 nm air gaps for use as notch filters in nanodevices. To preserve the structural integrity of these devices for optical studies, we further coat them with silica. GMAIL studies of these coated wires clearly demonstrate the presence of a nanogap. In addition, we see guided luminescence at

the far end, which can be segregated from the luminescence at the gap. The efficiency of free photons released at the far end in the gap wires is dependent on the position of the gap in the wire. We are currently obtaining luminescence spectra from the excited end, the distal end, and the gaps of such wires to demonstrate their notch filter behavior.

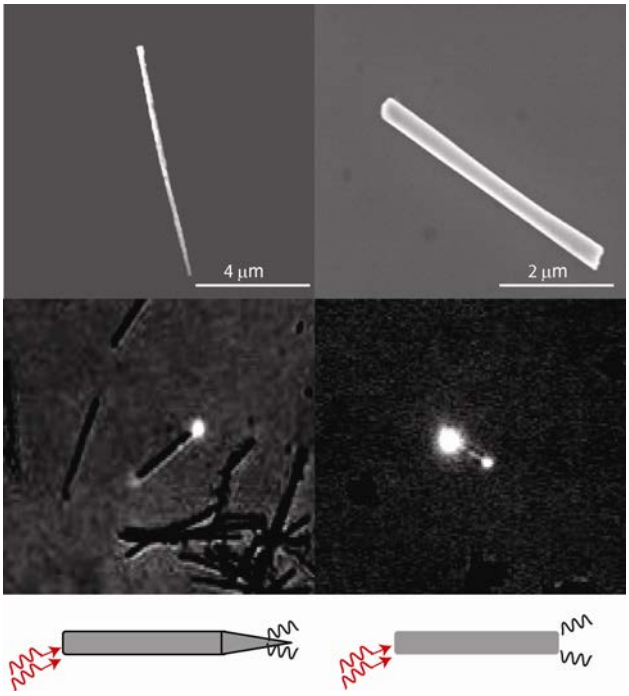

Figure 1 : Left Panel: (Top) SEM image of a tapered silver nanowire. (Bottom) Far-field excitation characteristic of a tapered nanowire. Right Panel: (Top) SEM image of a uniform-diameter silver nanowire. (Bottom) Far-field excitation characteristics of a uniform nanowire.

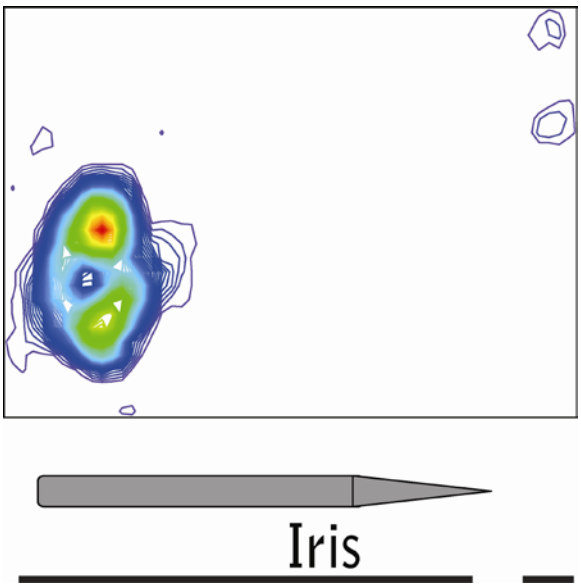

Figure 2 : Far-field excitation image of a tapered silver nanowire. The guided luminescence is isolated by the iris.

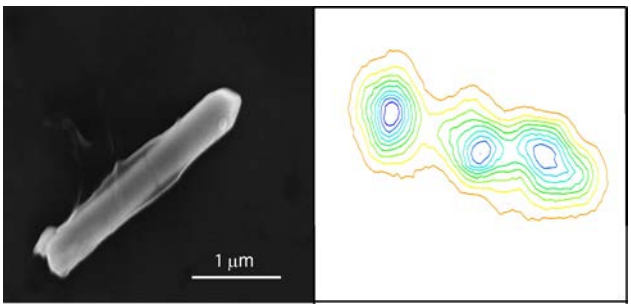

Figure 3 : (Left) SEM of an silver nanowire with a nanogap . (Right). Far-field excitation image of a similar silver nanowire**.**

Simulation and theory

Under this grant we endeavored to measure the effective impedance of an abruption in a nanorod waveguide at optical frequencies. Such an abruption, if properly designed, may appear as a lumped circuit element such as a capacitor, inductor, or resistor. Just as has been done in the RF domain, these basic building blocks of electronic circuit design can then be combined to form much more complicated circuits such as deeply subwavelength filters.

In the microwave domain a common technique to measure the effective impedance of an element is through the use of the standing wave ratio and the position of the nulls using a device known as a slotted line. In this way a complex reflection coefficient can be found with only power measurements. The technique parallels nicely to the use of a Near-Field Scanning Microscope (NSOM) in which a tapered optical fiber is scanned across a sample to measure the local optical fields. Additionally, this also parallels a much newer technique using quantum dots, which interact incoherently with their surroundings. Quantum dots (QD) have an advantage over traditional Near-Field Scanning Microscopes (NSOMs) in that the probe is inherently very small and perturb the optical fields only slightly. The strategy is to scan an emitting QD up and down the length of a nanorod using fluidic control while observing the light being scattered from each end. This differs slightly from the traditional use of a slotted line and NSOM in that the role of source and detector has been switched, however, through reciprocity in many cases this difference changes little.

We, therefore, sought to answer several questions:

Is it possible to recover known results?

In microwave engineering, calibration standards are used to determine the quality of a test apparatus. The common "short" forces the electric field to be zero at an interface so that there is a field null at the boundary while the "open" forces the current to be zero so that there is an electric field maximum at the boundary. Approximately analogous to an "open" is a simple nanorod end. As shown in Figure 1, in simulation we verify that this can be recovered by scanning a probe (in this case an NSOM tip in our simulation) down the length of the rod while the rod is being illuminated by a dipole at one end. At each point a broadband spectroscopic signal is acquired. These spectrums are compiled so that the behavior of each wavelength can be examined point by point. The data is fitted to a model which includes a complex propagation constant and a complex reflection coefficient. Indeed, we find that for longer wavelengths where the rod is more "wire-like" the reflected wave from the "open" end of the wire originates with a phase and amplitude similar to that of a microwave "open."

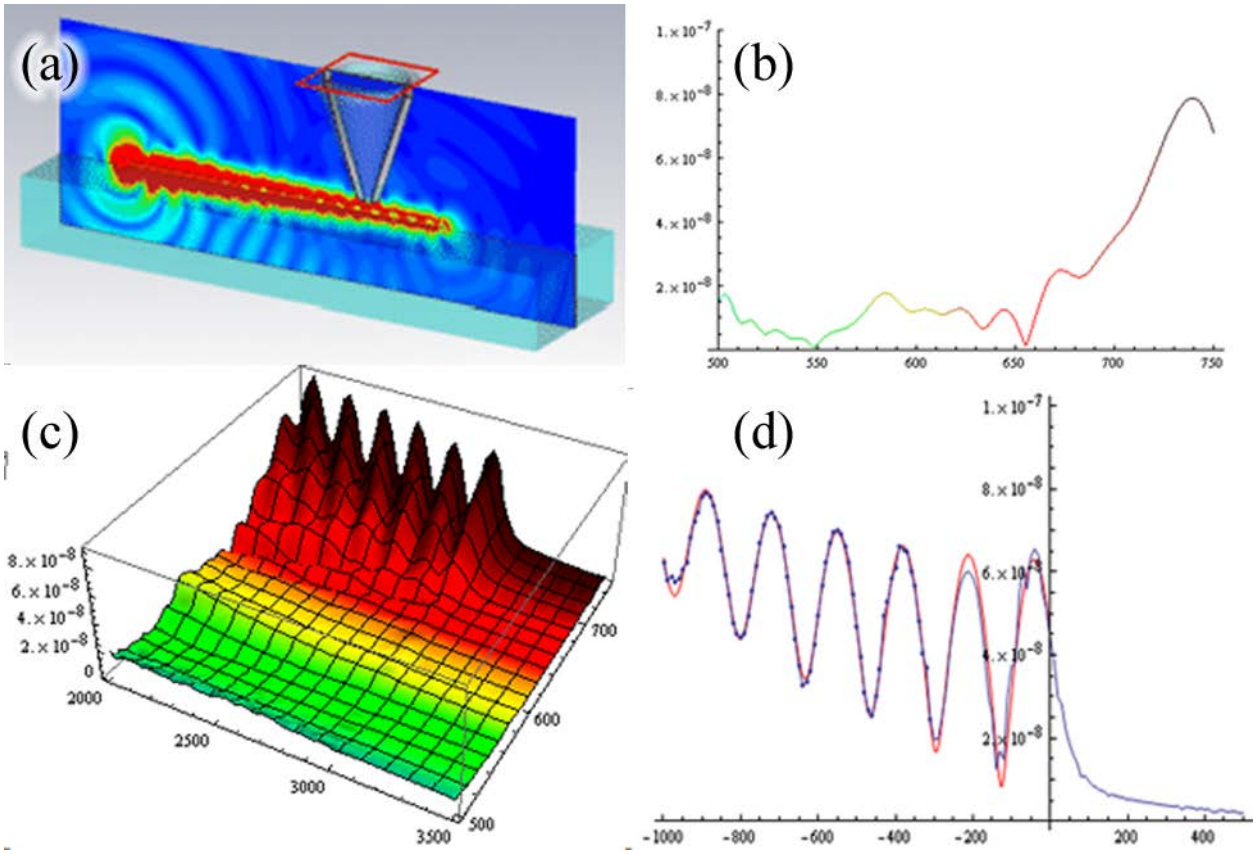

Figure 1: Simulation results: Broadband Scanning Procedure Using an NSOM. (a) In this simulation, the NSOM tip is scanned down the length of the rod which is illuminated using a broadband source. (b) At each point a power spectrum is taken. (c) Taking the spectral information at each point allows us to examine what happens at a particular wavelength. (d) The data is fitted to a forward and backward propagating wave with a complex reflection coefficient.

How does a traditional NSOM tip obfuscate the results?

In Figure 2, we show the simulation results for a silver nanorod on a glass substrate illuminated by a dipole at one end with wavelength of 633nm. The wave travels down the rod. In one case the NSOM probe tip is brought within 50nm of the rod while in the other it is brought within 10nm. In the second case, a substantial standing wave is clearly evident in front of the NSOM tip indicating that the tip is causing interference and causing reflections. NSOMs maintain their height using the same techniques employed by Atomic Force Microscopes, and it is very likely that the latter case is closer to the experimental reality. This is one of the reasons that it was better to use of QDs as our primary technique for reflection coefficient extraction.

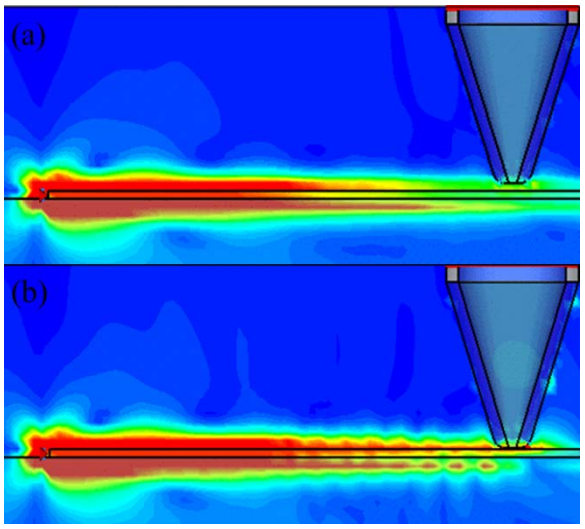

Figure 2: Simulation results: NSOM Tip Effect. Magnitude of electric field when tip is (a) 50nm and (b) 10nm above a 50nm silver nanorod illuminated at 633nm.

Under what conditions will the nanorod be monomodal so that the abruption can be described as a simple two port network?

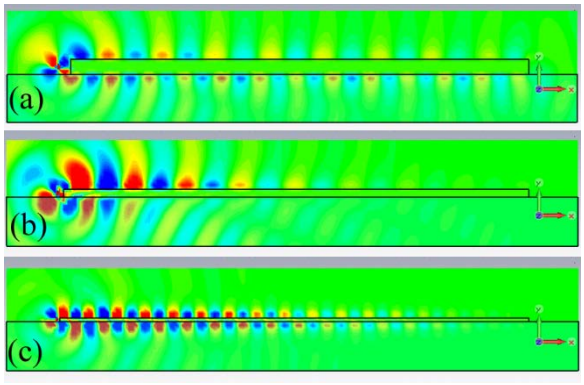

Figure 3: Simulation results: Effect of nanorod diameter on mode behavior of a (a) 200nm (b) 100 nm and (c) 50nm nanorod on a glass substrate in air.

Waveguides can often support more than one mode, each of which function independently of each other. The measured fields are then the sum of these modes. It severely complicates extraction of complex reflection coefficients when there are several modes present. In an NSOM based technique the nanorod will be on a glass substrate exposed to air. It is apparent from Figure 3 that it is necessary to have small diameter wire in order for the substrate to not cause the mode to split into an upper (fast) mode and a lower (slow) mode. Unfortunately, this small diameter also increases losses.

In the microfluidic controlled QD probe technique, the nanorods are in suspension in water (n=1.33) and settle down to the surface of PDMS substrate (n=1.40). The QD's are small enough to stay in suspension and so must be kept in the same plane as the nanorod through the use of a water/resin clamping layer (n=1.39) which can have tunable thickness. Over forty simulations were performed for different wavelengths and clamping layer thicknesses. However the results can be summarized to indicate that all wavelengths greater than 650nm were monomodal on a 100nm silver nanorod regardless of clamping layer thickness. However it was advantageous to have the clamping layer thickness be also 100nm to create a vertical symmetry which suppressed the creation of an upper and lower mode.

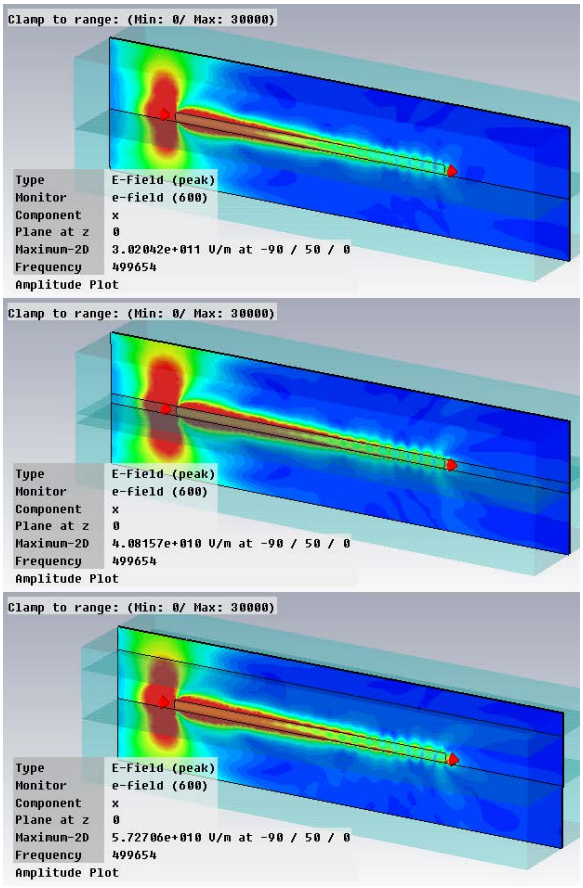

Figure 4: Simulation results: Mode behavior for 100nm Silver nanorod with no clamping layer (top panel), 100nm clamping layer (middle panel), and 500nm clamping layer (bottom panel) illuminated at 550nm

Can reciprocity be used to equate the source and sensor?

The vast majority of our simulations were of a nanorod excited at one end by a dipole, with the magnitude of the electric field plotted along the length of the nanorod. However, the actual experiments are opposite this with the source (i.e. the QD) being scanned down the length of the rod while observing the light scattered from the nanorod end. The QD will couple to the nanorod with an efficiency proportional to the local electric field of that mode and so there is an equivalence that can be drawn related to Purcell enhancement and reciprocity. However, it is computationally much more expensive to simulate a moving source than a stationary one. Theory aside, it is reassuring to see almost identical results in theory and experiment. Therefore, in simulation we scanned a QD along the length of a nanorod and plotted the total power radiated toward the microscope objective. The resulting picture is remarkably similar to what was observed in experiment. As the QD is scanned along the length of the nanorod, the emission from the nanorod ends clearly oscillates

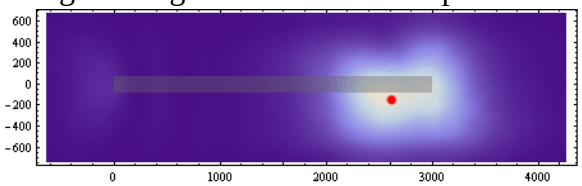

Figure 5: Simulation of a QD (red dot) next to a 100nm diameter, 3um silver nanorod as observed through a microscope objective.

indicating the standing wave patterns of that mode at the QD location.